



HAL
open science

COMPUTATION OF AVOIDANCE REGIONS FOR DRIVER ASSISTANCE SYSTEMS BY USING A HAMILTON-JACOBI APPROACH

Ilaria Xausa, Robert Baier, Olivier Bokanowski, Matthias Gerdts

► **To cite this version:**

Ilaria Xausa, Robert Baier, Olivier Bokanowski, Matthias Gerdts. COMPUTATION OF AVOIDANCE REGIONS FOR DRIVER ASSISTANCE SYSTEMS BY USING A HAMILTON-JACOBI APPROACH. 2015. hal-01123490v1

HAL Id: hal-01123490

<https://hal.science/hal-01123490v1>

Preprint submitted on 5 Mar 2015 (v1), last revised 27 Nov 2019 (v3)

HAL is a multi-disciplinary open access archive for the deposit and dissemination of scientific research documents, whether they are published or not. The documents may come from teaching and research institutions in France or abroad, or from public or private research centers.

L'archive ouverte pluridisciplinaire **HAL**, est destinée au dépôt et à la diffusion de documents scientifiques de niveau recherche, publiés ou non, émanant des établissements d'enseignement et de recherche français ou étrangers, des laboratoires publics ou privés.

COMPUTATION OF SAFETY REGIONS FOR DRIVER ASSISTANCE SYSTEMS BY USING A HAMILTON-JACOBI APPROACH

ILARIA XAUSA, ROBERT BAIER, OLIVIER BOKANOWSKI,
AND MATTHIAS GERDTS

ABSTRACT. We consider the problem of computing safety regions, modelled as backward reachable sets, for a car collision avoidance model with time-dependant obstacles. The Hamilton-Jacobi-Bellman framework is used, following the approach of Bokanowski and Zidani (Proceeding IFAC 2011, Vol. 18, Part 1, pp. 2589–2593). Furthermore several practical issues for specific obstacle avoidance problems are answered in this work. Different scenarios are then studied and computed. Comparison with a more direct optimal control approach is also done in the case of fixed obstacles. Computations involve solving nonlinear Partial Differential Equations up to five space dimensions plus time and for non smooth data, and an efficient solver is used to this end.

Keywords: safety avoidance, collision avoidance, Hamilton-Jacobi equations, backward reachable sets, level set approach, Partial Differential Equations, high dimension

1. MOTIVATION

The paper investigates optimal control approaches for the detection and indication of potential collisions in car motions. The aim is to identify and to compute safety regions for the car by means of a reachable set analysis for its underlying dynamics.

As first step, we need to define the optimal control problem obtained by modeling the motion of the car (described by ODEs and PDEs) and the environment where it lies (scenario set by state constraints and boundary constraints). A precise model (as the one in [12]) includes a pretty large number of states and highly non-linear differential equations. On the other hand models with less states and simpler equations (as the 4-dimensional model presented here) are easier to handle numerically. This is the reason why it is necessary to find a good compromise for the complexity of the model between affinity to the real behavior of the car and CPU times to compute a solution. Afterwards, once an obstacle has been detected by

Date: September 30, 2014.

This work was partially supported by the EU under the 7th Framework Programme Marie Curie Initial Training Network “FP7-PEOPLE-2010-ITN”, SADCO project, GA number 264735-SADCO.

suitable sensors (e.g. radar, lidar), the following approaches can be used to decide in the model whether a collision is going to happen or not. Firstly, we can compute the minimal time optimal trajectory to reach the safety target area avoiding the obstacles. Secondly, we look for the set of all initial point from which is possible to have an admissible solution. Both approaches are implemented for a software solving HJB equations [18], considering several car models and scenarios. The ROC-HJ Solver for solving Hamilton-Jacobi Bellman equations can be used for reachable sets computations and optimal trajectory reconstruction. Moreover we compare such simulations with the results obtained with a software using direct methods [13]. The package OCPID-DAE1 with a Fortran 90 interface is designed for the numerical solution of optimal control problems and parameter identification problems.

The plan of the paper is the following. In section 2, we consider the 4-dimensional point mass model for a car and describe the problem of the backward reachable set computation under different type of state constraints. In section 3, the HJB approach is briefly recalled in our setting. In section 4, a general (and simple) way to construct explicit level set functions associated to state constraints is introduced. Section 5 contains several numerical examples for collision avoidance scenarios, showing the relevance of our approach. Finally a conclusion is made in Section 6, where we also outline some ongoing works using the HJB approach for collision avoidance.

2. PROBLEM SETTING AND MODELLING

2.1. Presentation of the problem. The main tasks in collision avoidance are to reliably indicate future collisions and – if possible – to provide escape trajectories if such exist. In particular once an obstacle has been detected by suitable sensors (e.g. radar, lidar), we want to be able to decide whether a collision is going to happen or not. The technique presented here is based on the computation of the *backward reachable set*, which is the set of initial points from which the car can avoid an obstacle and reach a *safety target* Ω within a given time $t \geq 0$.

Let U be a nonempty compact subset of \mathbb{R}^m with $m \geq 1$. Let $n \geq 1$ and $f : \mathbb{R}^n \times U \rightarrow \mathbb{R}^n$ be Lipschitz continuous with respect to (z, u) . Let

$$\mathcal{U} := \{u : [0, \infty) \rightarrow U, u \text{ measurable}\}$$

be the set of control policies. Given an initial state $z_0 \in \mathbb{R}^n$, we denote by $z_{z_0}^u$ the *absolutely continuous* solution of the following dynamical system

$$\dot{z}(s) = f(z(s), u(s)) \quad \text{for a.e. } s \geq 0, \quad (1)$$

$$z(0) = z_0. \quad (2)$$

Let Ω and $(\mathcal{K}_s)_{s \geq 0}$ be nonempty closed sets of \mathbb{R}^n . The *backward reachable set reaching the target* Ω *within time* t associated to the dynamics f is defined

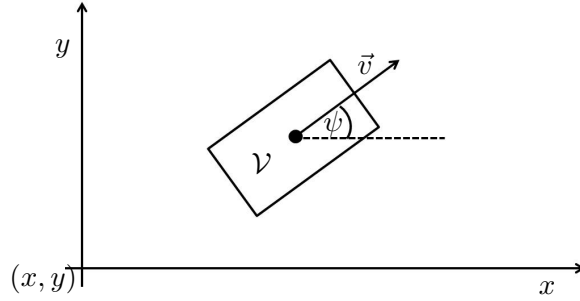


FIGURE 1. Vehicle and obstacles

as:

$$\mathcal{R}_t^f := \left\{ z_0 \in \mathbb{R}^n \mid \exists \tau \in [0, t], \exists u \in L^\infty([0, \infty), U) : z_{z_0}^u(\tau) \in \Omega \right. \\ \left. \text{and } z_{z_0}^u(s) \in \mathcal{K}_s \text{ for } s \in [0, \tau] \right\}$$

2.2. The 4-dimensional point mass model. The *point mass model* is a simplified four-dimensional state model for the car, where the controls are the acceleration and the steering angle velocity.

The center of gravity of the car is identified with its coordinates $(x(t), y(t))$, $v(t)$ denotes the module of the velocity of the car and $\psi(t)$ is the steering angle, see Fig. 1. The equations of motion are then given by

$$x' = v \cos(\psi) \quad (3a)$$

$$y' = v \sin(\psi) \quad (3b)$$

$$\psi' = w \quad (3c)$$

$$v' = a \quad (3d)$$

where $a(t) \in [a_{min}, a_{max}]$ is the control for acceleration (if $a(t) > 0$) and/or braking (if $a(t) < 0$), and $w(t)$ is steering angle velocity, such that $|w(t)| \leq w_{max}$. A description and an application of a more complete 7-dimensional model to two scenarios for collision avoidance on a straight road can be found in [19].

2.3. Level set functions for target and state constraints. The *target set* Ω will represent the safety area. In our examples we will take a region in the form of

$$\Omega = \left\{ z = (x, y, \psi, v) \in \mathbb{R}^4 \mid x \geq x_{target}, y \geq y_{target}, |\psi| \leq \varepsilon \right\} \quad (4)$$

for a small threshold $\varepsilon > 0$.

An important tool that will be used in this paper is the notion of *level set functions* associated to a given set. For the target constraint Ω , we will

associate a Lipschitz continuous function $\varphi : \mathbb{R}^n \rightarrow \mathbb{R}$ (here with $n = 4$), such that

$$z \in \Omega \iff \varphi(z) \leq 0.$$

Indeed there always exists such a function, since one can use the *signed distance* to Ω ($\varphi(z) = d(z, \Omega)$ if $z \notin \Omega$, and $\varphi(z) = -d(z, \mathbb{R}^n \setminus \Omega)$ if $z \in \Omega$). But it is in general easy to construct simple level set functions. For instance, in the case of (4), we can consider:

$$\varphi(z) := \max \left(-(x - x_{target}), -(y - y_{target}), |\psi| - \varepsilon \right).$$

Now for the case of the state constraints, different road geometries will be considered, as well as different fixed and/or moving obstacles that the car must avoid. In all cases, we will manage to model all state constraints by a simple, explicit, level set function g .

In the particular case of fixed configurations, state constraints are of the form $z(s) \in \mathcal{K}$ for all $s \in [0, t]$ (for a given closed set \mathcal{K} of \mathbb{R}^n), and we will construct a Lipschitz continuous function $g : \mathbb{R}^n \rightarrow \mathbb{R}$ such that

$$z \in \mathcal{K} \iff g(z) \leq 0.$$

In the general case of moving obstacles, the state constraints are of the form

$$z(s) \in \mathcal{K}_s, \quad \forall s \in [0, t],$$

where $(\mathcal{K}_s)_{s \geq 0}$ is a family of closed sets. Then we need to introduce a time-dependent level set function (still denoted g) $g : \mathbb{R}^n \times \mathbb{R} \rightarrow \mathbb{R}$, such that, for any $s \geq 0$,

$$z \in \mathcal{K}_s \iff g(z, s) \leq 0.$$

The obstacles and corresponding level set functions will be more precisely described and constructed in Section 4.

3. HAMILTON-JACOBI-BELLMAN APPROACH

The following assumptions (H1)-(H4) will be needed:

- (H1) $f : \mathbb{R}^n \times U \rightarrow \mathbb{R}^n$ is a continuous function and Lipschitz continuous in z uniformly in u , i.e. $\exists L \geq 0, \forall z_1, z_2, \forall u \in U: |f(z_1, u) - f(z_2, u)| \leq L|z_1 - z_2|$.
- (H2) For all $z \in \mathbb{R}^n$ the velocity set $f(z, U)$ is convex.
- (H3) Ω is a nonempty closed set of \mathbb{R}^n . Let $\varphi : \mathbb{R}^n \rightarrow \mathbb{R}$ be Lipschitz continuous and a level set function for the target, i.e.

$$\varphi(z) \leq 0 \iff z \in \Omega.$$

- (H4) $(\mathcal{K}_s)_{s \in [0, T]}$ are a family of subsets of \mathbb{R}^n such that there exists a Lipschitz continuous level set function $g : \mathbb{R}^n \times \mathbb{R} \rightarrow \mathbb{R}$ with

$$g(z, s) \leq 0 \iff z \in \mathcal{K}_s \quad \text{for all } s \in [0, T], z \in \mathbb{R}^n.$$

We now focus on backward reachable sets associated to a dynamics f and how to compute such reachable sets.

Definition 3.1. The *backward reachable sets reaching the target Ω at times $\tau \leq t$* for the dynamics f with time-dependent sets (\mathcal{K}_s) for the state constraints is defined by

$$\mathcal{R}_t^f := \left\{ z_0 \in \mathbb{R}^n \mid \exists \tau \in [0, t], \exists u \in \mathcal{U} : z_{z_0}^u(\tau) \in \Omega \right. \\ \left. \text{and } z_{z_0}^u(s) \in \mathcal{K}_s \text{ for all } s \in [0, \tau] \right\}. \quad (5)$$

Remark 3.1. Let the *capture bassin* be defined by

$$\text{Cap}_{\Omega, (\mathcal{K}_s)}^f(t) := \left\{ z_0 \in \mathbb{R}^n \mid \exists u \in \mathcal{U}, z_{z_0}^u(t) \in \Omega \right. \\ \left. \text{and } z_{z_0}^u(s) \in \mathcal{K}_s \text{ for all } s \in [0, t] \right\} \quad (6)$$

(following in particular [1, Subsec. 1.2.1.2]). When there is no time dependency, $(\mathcal{K}_s) = \mathcal{K}$, it is known that the set (5) is a capture basin:

$$\mathcal{R}_t^f \equiv \text{Cap}_{\Omega, \mathcal{K}}^{\tilde{f}}(t)$$

associated with the dynamics $\tilde{f}(z_0, (u, \lambda)) := \lambda f(z_0, u)$ for $(u, \lambda) \in \tilde{U} = U \times [0, 1]$ (see for instance [16]). Here, a new virtual control $\lambda(\cdot)$ with $\lambda(s) \in [0, 1]$ is introduced.

Now let the *value function v* be defined by

$$v(z_0, t) := \inf_{u \in \mathcal{U}} \max \left(\varphi(z_{z_0}^u(t)), \max_{s \in [0, t]} g(z_{z_0}^u(s)) \right),$$

where we simply denote $g(z, s) \equiv g(z)$ in the case $\mathcal{K}_s \equiv \mathcal{K}$. Such value function involving a supremum cost have been studied by Barron and Ishii in [5]. Then the function v is a level set function for $\text{Cap}_{\Omega, \mathcal{K}}^{\tilde{f}}(t)$ in the sense that the following holds (see [6])

$$\text{Cap}_{\Omega, \mathcal{K}}^{\tilde{f}}(t) = \{z_0 \in \mathbb{R}^n \mid v(z_0, t) \leq 0\}. \quad (7)$$

In particular assumptions (H3) and (H4) are essential for (7) to hold. Furthermore, v is the unique continuous *viscosity solution* (in the sense of [4]) of the following Hamilton-Jacobi (HJ) equation

$$\min \left(\partial_t v + \mathcal{H}(z, \nabla_z v), v - g(z) \right) = 0, \quad t > 0, z \in \mathbb{R}^n, \quad (8a)$$

$$v(z, 0) = \max(\varphi(z), g(z)), \quad z \in \mathbb{R}^n, \quad (8b)$$

where

$$\mathcal{H}(z, p) := \max_{u \in U} (-f(z, u) \cdot p), \quad p \in \mathbb{R}^m,$$

is the *Hamiltonian*.

For the computation of backward reachable sets with time dependent state constraints, we will follow the approach of [7]. We consider the new state variable $\xi := (z, s)$ and the "augmented" dynamics with values in \mathbb{R}^5 :

$$F(\xi, u) := \begin{pmatrix} f(z, u) \\ 1 \end{pmatrix}. \quad (9)$$

Let also be $\xi_0 := (z_0, t_0)$ and trajectories $\xi_{\xi_0}^u$ associated to F , fulfilling

$$\dot{\xi}(s) = F(\xi(s), u(s)) \text{ and } \xi(0) = \xi_0.$$

For a fixed $T > 0$, let

$$\tilde{\Omega} := \bigcup_{s \in [0, T]} \Omega \times \{s\} \equiv \Omega \times [0, T] \quad (10)$$

and

$$\tilde{\mathcal{K}} := \bigcup_{s \in [0, T]} \mathcal{K}_s \times \{s\}. \quad (11)$$

Then it holds:

Proposition 3.2. *For all $t \geq 0$, we have:*

$$\forall s \in [0, t], z_0 \in \text{Cap}_{\Omega, (\mathcal{K}_s)}^f(t) \iff (z_0, 0) \in \text{Cap}_{\tilde{\Omega}, \tilde{\mathcal{K}}}^F(t).$$

We extend the definition of φ by $\varphi(z, s) := \varphi(z)$ so that for any $\xi_0 \in \mathbb{R}^n \times \mathbb{R}$ and $\tau \geq 0$ we can associate a value w as follows:

$$w(\xi_0, \tau) := \inf_{u \in \mathcal{U}} \max \left(\varphi(\xi_{\xi_0}^u(\tau)), \max_{s \in [0, \tau]} g(\xi_{\xi_0}^u(s)) \right)$$

Then, one can verify that w is Lipschitz continuous and the following theorem holds:

Theorem 3.3. *Assume (H1)-(H4).*

(i) *For every $\tau \geq 0$ we have:*

$$\text{Cap}_{\Omega, (\mathcal{K}_s)}^f(\tau) = \{z \in \mathbb{R}^n, w((z, 0), \tau) \leq 0\}.$$

(ii) *w is the unique continuous viscosity solution of*

$$\min(\partial_\tau w + \mathcal{H}((z, t), (\nabla_z w, \partial_t w)), w((z, t), \tau) - g(z)) = 0, \quad \tau > 0, (z, t) \in \mathbb{R}^{n+1} \quad (12a)$$

$$w((z, t), 0) = \max(\varphi(z), g(z, t)), \quad (z, t) \in \mathbb{R}^{n+1}. \quad (12b)$$

where for any $\xi = (z, t)$ and $(p_z, p_t) \in \mathbb{R}^n \times \mathbb{R}$:

$$\mathcal{H}((z, t), (p_z, p_t)) := \max_{u \in U} (-f(z, u) \cdot p_z - p_t).$$

Once the backward reachable set is characterized by a viscosity solution of (12), it is possible to use a PDE solver to find the solution on a grid.

Minimal time function and optimal trajectory reconstruction. In the case of fixed state constraints (i.e. $\mathcal{K}_s \equiv \mathcal{K}$), the *minimal time function*, denoted by \mathcal{T} , is defined by:

$\mathcal{T}(z_0) := \inf\{t \in [0, T] \mid \exists u \in \mathcal{U} : z_{z_0}^u(t) \in \Omega \text{ and } z_{z_0}^u(s) \in \mathcal{K} \text{ for all } s \in [0, t]\}$, and if no such time t exists then we set $\mathcal{T}(z_0) = \infty$. It is easy to see that the function satisfies

$$\mathcal{T}(z_0) = \inf\{t \in [0, T], v(z_0, t) \leq 0\}.$$

Notice that \mathcal{T} can be discontinuous even though v is always Lipschitz continuous. No controllability assumptions are used in the present approach.

The optimal trajectory reconstruction is then obtained by minimizing the minimal time function along possible trajectories (see for instance Falcone [9]). More precisely, assume that the starting point is z_0 and that we aim to reach $z_n := z^u(t_n) \in \Omega$ at some future time $t_n > 0$. This is equivalent to require $\mathcal{T}(z_n) = 0$. For a given small threshold $\eta > 0$, for a given control discretization of the set U , say $(u_k)_{k=1, \dots, N_u} \subset U$, and $t_n := n\Delta t$ for a given time step $\Delta t > 0$, we consider the following iterative procedure:

while $n < N$ and $\mathcal{T}(z_n) \geq \eta$ do:
 Find $k^* := \operatorname{argmin}_{k=1, \dots, N_u} \mathcal{T}(\bar{z}_{z_n}^{u_k}(\Delta t))$
 Set $z_{n+1} := \bar{z}_{z_n}^{u_{k^*}}(\Delta t)$
 $n := n + 1$

where $\bar{z}_{z_n}^{u_k}(h)$ denote a *one-step second-order Runge-Kutta approximation* of the trajectory with fixed control u_k on $[t_n, t_{n+1}]$. The *Heun scheme with piecewise constant selections* uses the iteration:

$$\bar{z}_{z_n}^{u_k}(h) := z_n + \frac{h}{2}(f(z_n, u_k) + f(z_n + hf(z_n, u_k), u_k)).$$

It is also possible to do smaller time steps between $[t_n, t_n + \Delta t]$ in order to improve the precision for a given control u_k . Nevertheless, numerical observations are showing that the approximation is in general more sensitive to the control discretization $(u_k)_{k=1, \dots, N_u}$ of the set U .

In the time-dependent case this minimal time function can be defined in a similar way from the value w (we refer to [7] for details), and the optimal trajectory reconstruction follows the same lines with the "augmented" dynamics (9).

4. LEVEL SET FUNCTIONS FOR DIFFERENT ROAD CONFIGURATIONS

4.1. Road configurations. Let us first describe different simple road geometries depicted in Fig. 2 that will be used in the next numerical section. The road will be denoted \mathcal{K}_r , a subset of \mathbb{R}^2 .

- A straight road with constant width:

$$\mathcal{K}_r = \left\{ (x, y) \in \mathbb{R}^2 \mid y_{down} \leq y \leq y_{up} \right\}, \quad (13)$$

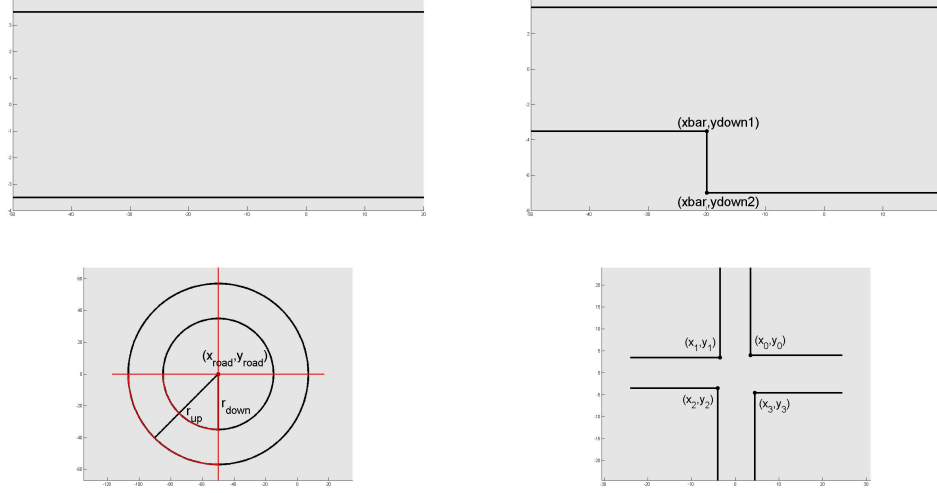


FIGURE 2. Different road geometries: straight (top-left), varying width (top-right), curved (bottom-left), crossing (bottom-right).

with $y_{down} = -3.5$ and $y_{up} = 3.5$ (values are typically in meters). A level set function associated to \mathcal{K}_r can be given by

$$g(x, y) := \max \left(-(y - y_{down}), -(y_{up} - y) \right). \quad (14)$$

- A straight road with varying widths, modeled as:

$$\mathcal{K}_r := \left\{ (x, y) \in \mathbb{R}^2 \mid y_{down}(x) \leq y \leq y_{up} \right\}, \quad (15)$$

where

$$y_{down}(x) = \begin{cases} y_{down_1} & \text{if } x \leq \bar{x}, \\ y_{down_2} & \text{if } x > \bar{x}. \end{cases} \quad (16)$$

$y_{up}, y_{down_1}, y_{down_2}, \bar{x}$ constants. It would be natural to define the level set function of (15) as in (14) where instead of y_{down} we use the function $y_{down}(x)$ defined in (16). However, (16) leads to a discontinuous function g , which is not convenient for our purposes. In this particular case, the following definition is better suited because it is Lipschitz continuous in (x, y) :

$$g(x, y) = \max \left(\min \left(-(y - y_{down_1}), -(x - \bar{x}) \right), \right. \\ \left. -(y - y_{down_2}), (y - y_{up}) \right). \quad (17)$$

- The circular curve shown in Figure 2, defined as

$$\mathcal{K}_r = \{(x, y), \theta_{\min} \leq \Theta(x, y) \leq \theta_{\max}, r_{\text{down}} \leq \rho(x, y) \leq r_{\text{up}}\} \quad (18)$$

where $\theta_{\min} < \theta_{\max}$ are two limiting angles for the road boundaries, (x_r, y_r) denotes the center of the road circle, $0 < r_{\text{up}} < r_{\text{down}}$ the radius of the bigger and smaller circle respectively, $\rho(x, y) := \sqrt{(x - x_c)^2 + (y - y_c)^2}$, $\theta = \Theta(x, y) \equiv \arctan(\frac{y - y_c}{x - x_c}) + k_{x,y}\pi$ (with $k_{x,y} \in \mathbb{Z}$) denotes a continuous representation on \mathcal{K}_r such that $x - x_c = r \cos(\theta)$ and $y - y_c = r \sin(\theta)$. The level set function is defined as

$$g(x, y) = \max \left(\rho(x, y) - r_{\text{up}}, -(\rho(x, y) - r_{\text{down}}), \Theta(x, y) - \theta_{\max}, -(\Theta(x, y) - \theta_{\min}) \right). \quad (19)$$

Remark 4.1. A general and simple rule for constructing Lipschitz continuous level set functions is the following. Assume that g_1 (resp. g_2) are Lipschitz continuous level set functions for the set \mathcal{K}_1 (resp. \mathcal{K}_2), that is, $g_i(x) \leq 0 \Leftrightarrow x \in \mathcal{K}_i$, for $i = 1, 2$. Then

$$\max(g_1(x), g_2(x)) \leq 0 \Leftrightarrow x \in \mathcal{K}_1 \cap \mathcal{K}_2 \quad (20)$$

$$\min(g_1(x), g_2(x)) \leq 0 \Leftrightarrow x \in \mathcal{K}_1 \cup \mathcal{K}_2. \quad (21)$$

Hence $\max(g_1, g_2)$ (resp. $\min(g_1, g_2)$) is Lipschitz continuous and can be used as a level set function for $\mathcal{K}_1 \cap \mathcal{K}_2$ (resp. $\mathcal{K}_1 \cup \mathcal{K}_2$). Then more complex structures can be coded by combining (20) and (21). This is related to well-known techniques in computational geometry (see e.g. [10, 15])

- A crossing with corner points $(x_i, y_i)_{i=0,\dots,3}$: Let the upper right part be defined as $\mathcal{K}_0 := \{x - x_0 \leq 0 \text{ or } y - y_0 \leq 0\}$, and similarly, $\mathcal{K}_1 := \{y - y_1 \leq 0 \text{ or } -(x - x_1) \leq 0\}$ (upper left part), $\mathcal{K}_2 := \{-(x - x_2) \leq 0, \text{ or } -(y - y_2) \leq 0\}$ (lower left part), $\mathcal{K}_3 := \{-(y - y_3) \leq 0, \text{ or } x - x_3 \leq 0\}$ (lower right part).

Following remark (4.1), a level set function for $\mathcal{K} := \bigcap_{i=0,\dots,3} \mathcal{K}_i$ can be obtained by

$$g(x, y) = \max \left(\min(x - x_0, y - y_0), \min(y - y_1, -(x - x_1)), \min(-(x - x_2), -(y - y_2)), \min(-(y - y_3), x - x_3) \right), \quad (22)$$

More general ways to construct level set functions for roads delimited by polygonal lines could be obtained following similar ideas. Also let us mention that the modeling of the road boundaries via piecewise cubic polynomials or B-splines can be obtained as in [11].

4.2. Obstacles and corresponding level set functions. Next, $k \geq 1$ additional obstacles are considered (obstacles which are different from the road). There are modelled as disks or rectangles that the car has to avoid

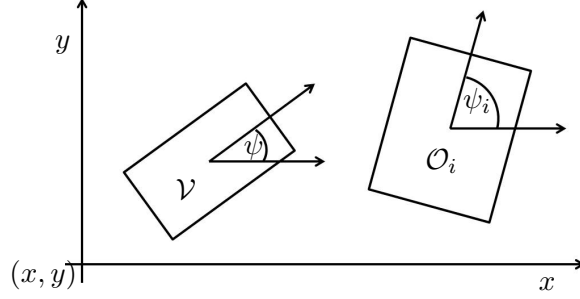


FIGURE 3. Vehicle and obstacles

(the car being itself modelled in the form of a disk or a rectangle), therefore defining an other type of state constraint.

Let $X_i = (x_i, y_i)$ denote the center of obstacle i , which may depend of the time s . Let $X = (x, y)$ denote the center of gravity of the vehicle.

Circular obstacles. We first consider the simpler case of circular obstacles and vehicle, where the vehicle is approximated by a closed ball $B(X, r)$ for a given $r > 0$, and the obstacles also by balls $B(X_i(s), r_i)$ centered at $X_i(s)$ and with given fixed radius $r_i > 0$. Then it holds $B(X_i(s), r_i) \cap B(X, r) = \emptyset \Leftrightarrow \|X - X_i(s)\|_2 > r + r_i$, hence there is no collision at time s if $B(X, r) \cap \bigcup_{1 \leq i \leq k} B(X_i(s), r_i) = \emptyset$, which amounts to saying

$$g(z, s) := \min_{1 \leq i \leq k} -(\|X - X_i(s)\|_2 - r - r_i) < 0, \quad (23)$$

where $z = (x, y, \psi, v)$.

Rectangular obstacles. We now turn on the more realistic case of rectangular obstacles and vehicle. We assume the vehicle V is a rectangle centered at X and with half lengths $\ell = (\ell_x, \ell_y)^T$. We assume that each obstacle \mathcal{O}_i is also a rectangle with center $X^i = X^i(s)$ and half lengths $\ell^i = (\ell_x^i, \ell_y^i)^T$. Then the four corners $(X_j)_{1 \leq j \leq 4}$ of the vehicle with state $z = (x, y, \psi, v)$ can be determined by

$$X_j = X + R_{-\psi} T_j \ell, \quad T_j = \begin{pmatrix} (-1)^{j-1} & 0 \\ 0 & (-1)^{\lfloor \frac{j-1}{2} \rfloor} \end{pmatrix}, \quad 1 \leq j \leq 4,$$

where $\lfloor x \rfloor$ denotes the integer part of a real x , and R_ψ denotes the rotation matrix $R_\psi := \begin{pmatrix} \cos(\psi) & -\sin(\psi) \\ \sin(\psi) & \cos(\psi) \end{pmatrix}$.

In the same way the four corners $(X_j^i)_{1 \leq j \leq 4}$ of obstacle \mathcal{O}_i (determined by its center $X^i(s)$ and orientation $\psi_i(s)$) are given by

$$X_j^i := X^i + R_{-\psi_i} T_j \ell^i, \quad 1 \leq j \leq 4.$$

Furthermore, for a given $X = (x, y)^T$, let

$$d_\ell(X) := \max(\ell_x - |x|, \ell_y - |y|).$$

The function d_ℓ is a level set function for the avoidance of $[-\ell_x, \ell_x] \times [-\ell_y, \ell_y]$, since $d_\ell(X) < 0 \Leftrightarrow X \notin [-\ell_x, \ell_x] \times [-\ell_y, \ell_y]$. For an arbitrary point $Y \in \mathbb{R}^2$, the following function

$$d_V(Y) := d_\ell(R_{-\psi}(Y - X))$$

is a level set function for the avoidance of the vehicle, in the sense that $d_V(Y) < 0 \Leftrightarrow Y \notin V$.

In the same way,

$$d_{\mathcal{O}_i}(Y) := d_{\ell^i}(R_{-\psi_i}(Y - X^i))$$

satisfies $d_{\mathcal{O}_i}(Y) < 0 \Leftrightarrow Y \notin \mathcal{O}_i$.

Now we consider for $z = (x, y, \psi, v) \in \mathbb{R}^4$ and $s \in \mathbb{R}$ the following function:

$$g(z, s) := \max_{1 \leq i \leq k} \left(\max_{j=1, \dots, 4} d_{V(z)}(X_j^i(s)), \max_{j=1, \dots, 4} d_{\mathcal{O}_i(s)}(X_j(z)) \right). \quad (24)$$

(if the obstacles positions do not depend of time we can define $g(z)$ in the same way without time dependency). Here we have denoted $V(z)$ and $X_j(z)$ for the vehicle position and corners to make clear the dependance in terms of the state variable z , and $X_j^i(s)$ to make clear the time dependency of the obstacle corners.

The function g will serve as a level set function for obstacle avoidance. Presently, from the definition of the g function, it holds:

Lemma 4.1. *The function g is Lipschitz continuous and*

$$g(z, s) < 0 \Leftrightarrow \forall i, j: X_j(z) \notin \mathcal{O}_i(s) \text{ and } \forall i, j: X_j^i(s) \notin V(z) \quad (25)$$

However, we aim to characterise the fact that the obstacle and vehicle are disjoint, i.e.,

$$V(z(s)) \cap \left(\bigcup_{1 \leq i \leq k} \mathcal{O}_i(s) \right) = \emptyset. \quad (26)$$

In general, the condition $g(z(s), s) < 0$ (that is, condition (25)) is not sufficient to ensure that (26) holds, as shown by the counter-example illustrated in Fig. 4.

In order to show that we will still be able to use condition (25) as a sufficient condition, we need furthermore the following result.

Lemma 4.2. *Assume at time $s = t_0$ condition (26) holds. Assume at time $s = t_1 > t_0$ condition (25) is fulfilled, but that (26) does not hold. Then*

$$t_1 - t_0 > \Delta t_0 := \underline{d}/\bar{v}$$

where d is the minimal car and obstacle lengths

$$\underline{d} := \min(\ell_x, \ell_y, \min_{1 \leq i \leq k} (\min(\ell_x^i, \ell_y^i)))$$

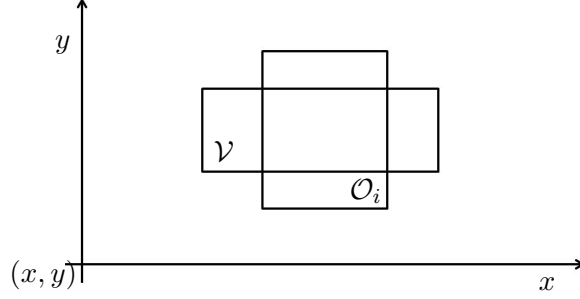


FIGURE 4. Example where vehicle and obstacle are not disjoint and $g(z(s), s) < 0$.

and v is an upper bound for all corner velocities (car and obstacles corners) involved in the computations:

$$\bar{v} := \max\left(\max_{1 \leq j \leq 4} \max_{s \in [0, T]} \|\dot{X}_j(s)\|, \max_{1 \leq i \leq k} \max_{1 \leq j \leq 4} \max_{s \in [0, T]} \|\dot{X}_j^i(s)\|\right). \quad (27)$$

Proof. This can be proved by using simple geometrical arguments. In the case a mixing occurs between the vehicle and one obstacle rectangle, then either one corner point of the vehicle will have run through the obstacle (therefore will have at least run a distance \underline{d} with maximum speed \bar{v}), or, conversely, one corner point of the obstacle will have run through the vehicle. \square

Notice that an upper bound of the quantity (27) can be obtained on a given computational bounded domain Ω and for given obstacle parameters.

From Lemma 4.1 and Lemma 4.2 we deduce

Proposition 4.3. *Assume that $\Delta t \in]0, \Delta t_0[$ where $\Delta t_0 := d/v$ is defined in Lemma 4.2. Let $t_1 = t_0 + \Delta t$. If condition (26) holds at time t_0 , and if $g(z(t_1), t_1) < 0$, then (26) also holds at time t_1 .*

In particular, when using the HJ PDE solver with time steps $t_n = n\Delta t$, if an initial time $t_0 = 0$ the vehicle and obstacle are disjoint (i.e. condition (26) holds) and if $0 < \Delta t < \Delta t_0$, then it suffices to verify

$$g(z(t_n), t_n) < 0, \quad n = 1, \dots, N,$$

(i.e., condition (25) at each successive time step) in order to guarantee that there is no collision, i.e.:

$$V(z(t_n)) \cap \left(\bigcup_{1 \leq i \leq k} \mathcal{O}_i(t_n) \right) = \emptyset \quad \forall n = 1, \dots, N.$$

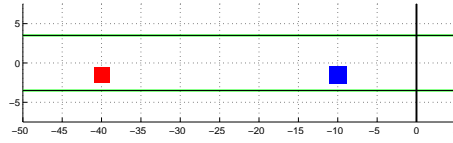


FIGURE 5. Car traffic scenario.

Moving obstacles. The possible motion for the obstacles that will be considered can either be a linear motion along a straight path:

$$x_i(s) = x_{i0} + v_{ix} s \quad (28a)$$

$$y_i(s) = y_{i0} + v_{iy} s \quad (28b)$$

$$\psi_{i0} = \arctan \frac{v_{iy}}{v_{ix}} \quad (28c)$$

where (v_{ix}, v_{iy}) is the constant velocity of the obstacle i and θ_{i0} is the initial angle which is constant during the motion. Or it can be a motion along a curved road,

$$x_i(s) = a \cos(\theta_{i0} + \omega_i s) + c_x, \quad (29a)$$

$$y_i(s) = a \sin(\theta_{i0} + \omega_i s) + c_y, \quad (29b)$$

$$\psi_{i0}(s) = (\theta_{i0} + \omega_i s) - \frac{\pi}{2}, \quad (29c)$$

where ω_i as a constant angular velocity.

5. NUMERICAL SIMULATIONS

Here we plot some numerical simulations for different scenarios. Throughout the paper, we use the 4-dimensional point mass model (3). In the present work and for solving the HJ equation (12), we have used a second order ENO finite difference scheme for partial differential equations of Hamilton-Jacobi type. (More precisely an ENO2 spatial discretization method as described in [17] is used, coupled with an Euler forward RK1 scheme in time). The computations have been performed by using the ROC-HJ parallel solver [18].

5.1. Scenario 1: straight road with a fixed rectangular obstacle.

We first consider a straight road configuration with only one fixed obstacle, as in Figure 5. The aim for the vehicle (represented by the red box) is to minimize the time to reach the safety region (the target, delimited by a blue line) and to avoid the obstacle (blue box). More precisely the parameters of the problem are:

- Vehicle parameters and initial position:
 $\ell_x = \ell_y = 1$ and $z_0 = (x_0, y_0, \theta_0, v_0) = \{-40.0, -1.5, 0.0, 35.0\}$
- Target: $\Omega = \{(x, y), x \geq 0, |y| \leq 3.5\}$.
- Obstacle parameters: one fixed obstacle with lengths $\ell_x^1 = \ell_y^1 = 1.0$ centered at $(x, y) = (-10.0, -1.5)$
- Road parameters: as described in (13) (straight road)

In Fig. 6 the reachable set is represented in blue and for different times. At time $t = 0$ only the points which are in the safety region (and away from the road boundary) are thus represented. Then the evolution of the (backward) reachable set is represented for different times. At time t_i , the region \mathcal{R}_{t_i} represent the set of starting points that can reach the target avoiding the obstacle within less than t_i seconds.

Next, in Fig. 7, we have represented the initial position of the vehicle as well as the optimal trajectory reconstruction : the car (red rectangle) drives from left to right in Fig. 7 and overtakes the fixed obstacle.

The white part in Fig. 7 corresponds to the area of starting points from which the blue car cannot reach the target, whatever maneuver is undertaken (mainly, its velocity is too high to avoid a collision with the blue car). Hence the trajectories from these points are infeasible, and such starting points do not belong to the backward reachable set.

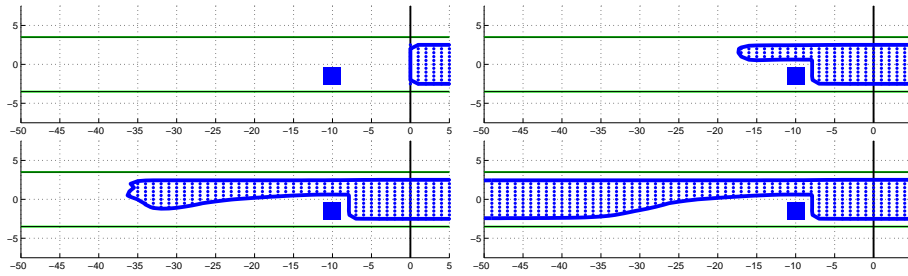


FIGURE 6. (Scenario 1) Reachable sets \mathcal{R}_{t_i} for different times ($t_1 = 0s, t_2 = 0.5s, t_3 = 1s, t_4 = 1.5s$)

Convergence test (scenario 1). For testing the stability of the HJ approach we first perform a convergence analysis with respect to mesh grid refinement. We define a grid on the state space

$$(x, y, \psi, v) \in [-50, 10] \times [-4, 4] \times [-1, 1] \times [5, 65],$$

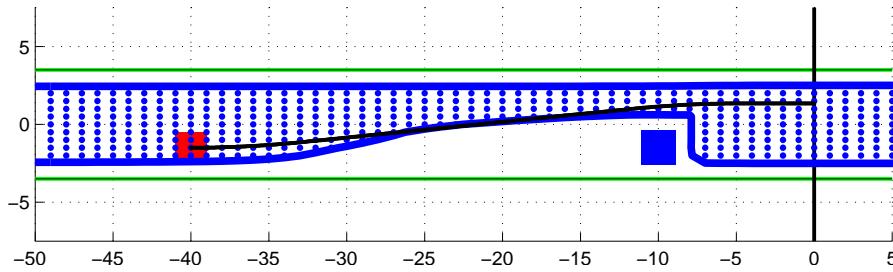


FIGURE 7. (Scenario 1) Reachable set \mathcal{R}_2^f , and optimal trajectory represented with a black line.

using a variable number of grid points in the (x, y) variables given by $N_x = 35 \cdot 2^m$ and $N_y = 4 \cdot 2^m$, depending on an integer parameter $m \in \{1, \dots, 5\}$. The number of grid points in the ψ and v variables are fixed and given by

$$N_\psi = 20 \quad \text{and} \quad N_v = 6.$$

The errors are computed by using a reference value function v_{ex} obtained for $m = 5$ (i.e., $N_x = 1020$, $N_y = 128$). Furthermore a CFL restriction of the type $\Delta t/\Delta x \leq \text{const}$ is used for the stability of the scheme. The results are given in Table 1. For a given grid mesh (z_i) and corresponding (constant) step space Δz , the local error at grid point z_i is $e_i := v(z_i) - v_{ex}(z_i)$ and the L^∞ , L^1 and L^2 errors are defined as follows:

$$e_{L^\infty} := \max_i |e_i|, \quad e_{L^1} := \Delta z \sum_i |e_i|, \quad e_{L^2} := \left(\Delta z \sum_i e_i^2 \right)^{1/2}.$$

In Table 1, in order to evaluate numerically the order of convergence for a given L^p norm, the estimate $\alpha_m := \frac{\log(e^{(m-1)}/e^{(m)})}{\log(2)}$ is used for corresponding values $N_x = 35 \cdot 2^m$ and $N_y = 4 \cdot 2^m$. (i.e. the mesh steps N_x and N_y are refined by 2 between two successive computations).

We observe a convergence of order roughly 2 even for the ENO2-RK1 scheme which in principle is only first order in time. This is due to the fact that the dynamics is close to a linear one in this case (we have also tested a similar RK2 scheme, second order in time, which gives similar convergence results on this example).

N_x	N_y	e_{L^∞}	order	e_{L^1}	order	e_{L^2}	order	CPU time (s.)
70	8	0.489	–	1.126	–	6.769	–	0.34
140	16	0.078	2.64	0.337	1.73	2.255	1.58	1.50
280	32	0.026	1.60	0.118	1.52	0.795	1.50	9.20
560	64	0.006	2.07	0.030	1.98	0.207	1.94	69.40

TABLE 1. (Scenario 1) Error table for varying (N_x, N_y) parameters.

Comparison with a direct method (scenario 1). In order to validate the HJB approach for this scenario, we have also compared the results with numerical simulations obtained by using a direct optimal control approach for calculating the reachable set. The simulations are obtained by using the OCPID-DAE1 Software [13], and following the approach described in [2, 3] and [14, 19]. The resulting backward reachable set within time $T = 2$ is plotted in Fig. 8 (upper graph) and is in good correspondence with the set obtained by the HJ approach (Fig. 8, lower graph). Notice that we can only expect that both computed reachable sets be equal up to some accuracy of the order $O(\Delta x)$ (with $\Delta x = 1$ in this figure).

Remark 5.1. The advantage of using a direct optimal control approach (like the OCPID-DAE1 Software) is that is able to deal with a greater number of

states variables, which is necessary whenever we need a precise car-model, close to the behavior of a real car. However the handling of state constraints (in particular obstacles with non-smooth boundaries) sometimes leads to numerical difficulties in order to get feasible trajectories.

On the other hand the PDE solver (like ROC-HJ for solving Hamilton-Jacobi equations) is limited, in practice, by the number of state variables, because it requires to solve a PDE with as many dimensions as the number of state variables. However if the dimension can be processed on a given architecture, then the HJ approach requests only the Lipschitz property of the functions describing the dynamics and the state constraints. In particular, there is no problem for dealing with non smooth obstacles such as rectangular obstacles, crossing roads scenarios (more generally it could handle polygonal roads or more complex polytopial obstacles).

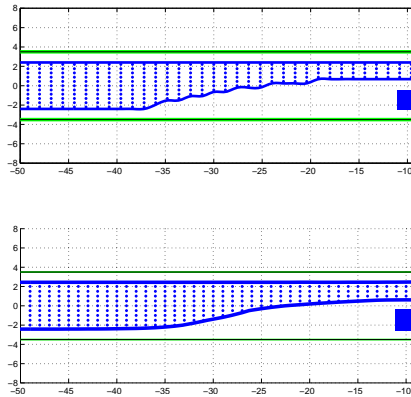


FIGURE 8. (Scenario 1) Comparison of reachable sets obtained with a direct method (up) and the HJ approach (down)

Next, we consider more complex scenarios and different road geometries.

5.2. Scenario 2: straight road with varying width. We shall consider a highway road with varying width :

$$\begin{cases} y_{up} = 3.5 \text{ m} \\ y_{down} = -3.5 \text{ m}, \text{ if } z_1 \leq -15.0 \\ y_{down} = -7.0 \text{ m}, \text{ if } z_1 > -15.0. \end{cases}$$

This is illustrated in Figs. (15) and (16) (the road is represented with green lines). This can be interpreted as an additional exit lane appearing only for a short part of the considered road.

Two obstacles (blue rectangles) are moving with linear motion (see (28)) in the same direction as the reference vehicle (red rectangle). All object widths and lengths are here equal to 1 m. The set of blue points depicted in

Figure 9 and Figure 10 is the projection on the (x, y) plane of the backward reachable set with $t_f = 2$ s, with steering angle $\psi(t_0) = 0$ rad and velocity $v(t_0) = 35$ m s⁻¹.

Scenario 2a: (see Fig. 9.) In this example an overtaking maneuver is considered with one first (obstacle) car in front of the vehicle, moving forward with velocity 10 m s⁻¹ and to be overtaken, and a second (obstacle) car next to the vehicle also moving forward at velocity 20 m s⁻¹ and blocking the maneuver. In Fig. 9, it is the position of the vehicle and of the obstacle cars that is shown at initial time $t_0 = 0$. (More precisely the parameters used for this Figure are $(N_x, N_y) = (70, 12)$ grid points; the trajectory (black line) is starting from $(x(0), y(0)) = (-40.0, -1.5)$, $\psi(0) = 0$ and $v(0) = 35$ m s⁻¹, a first obstacle car takes initial values $(x(0), y(0)) = (-10, -1.5)$, with $\psi(0) = 0$ and a constant velocity $v(0) = 10$ m s⁻¹; a second obstacle car takes initial values $(x(0), y(0)) = (-40, 1.5)$, with $\psi(0) = 0$ and a constant velocity $v(0) = 20$ m s⁻¹.)

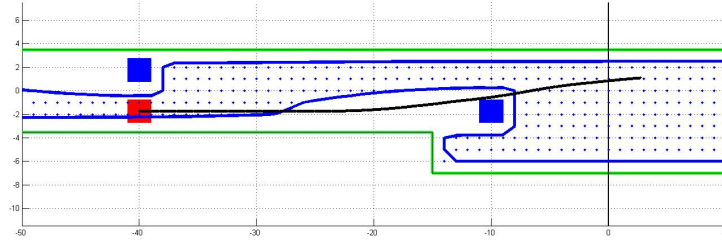


FIGURE 9. (Scenario 2a) Reachable set \mathcal{R}_2 .

Scenario 2b: (see Fig. 10.) This example is similar to the previous one excepted for the fact that the second (obstacle) car is next to the first one at initial time. (More precisely, the second obstacle car now takes initial values $(x(0), y(0)) = (-10, 1.5)$, and other parameters are otherwise unchanged).

The backward reachable set is the set of initial points of \mathbb{R}^4 (according to the model (3)) for which the collision can be avoided avoidable, and target can be reached, within t_f seconds (therefore so that is satisfied the final conditions $x(t_f) \geq 0$ and $\psi(t_f) = 0$). The set of blue points depicted in Figure 10 and Figure 9 is the projection on the (x, y) plane of the backward reachable set where the steering angle and the velocity are fixed to the values $\psi(t_0) = 0$ rad and $v(t_0) = 35$ m/s (which correspond to the initial values of the car when maneuver starts).

By starting in the blue region, the vehicle (in red) can avoid a collision. On the other hand, starting from a point in the white area then the vehicle

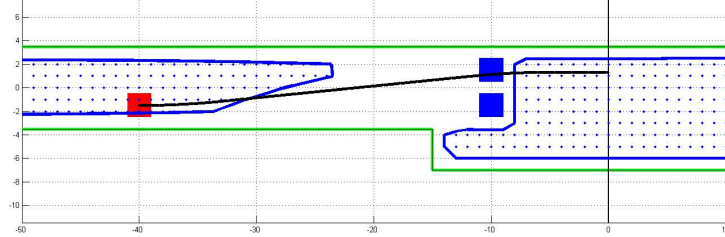


FIGURE 10. (Scenario 2b) The reachable set \mathcal{R}_2 is non connected to the contrary to scenario 2a.

will either go outside the road or will collide with the obstacle, before being able to reach the safety region.

In both figures we notice an extra part of the backward reachable set that lay below second obstacle. This is due to the varying road width, and means that the vehicle is forced to stay on the road.

In Figure (10) the backward reachable set is not connected, which means that the red rectangle can avoid a collision by starting the maneuver either leaving the obstacles behind (since it is faster no crash will occur) or from a sufficiently high distance behind the two obstacles depending on its y position (about 24 m if the reference vehicle starts in the first lane and 14 m if it starts in the second lane).

The optimal trajectories (black line) seem to overlap the obstacles and their trajectories before reaching the target set. This is because the blue rectangles only show the initial position of the obstacles at time t_0 , and not the evolution of their linear motion in the time interval $[t_0, t_f]$.

5.3. Scenario 3: curved road with fix or moving obstacles. The road shape is now described by the set of equations (18), with a 7 m width and a road radius of 50 m ; the boundaries of the road as shown by green lines in Figure 11.

Scenario 3a: Two fixed obstacles (blue rectangles with different width and length parameters) have to be avoided by the vehicle (red square), see Fig. 11, and the target $x \geq 0, \psi = 0$ has to be reached, if possible, in the time interval $[0, 5]$ seconds. The first obstacle has dimensions 0.5 m and is positioned in $(-5, 48.25)$. The second obstacle has width 0.5 m and length 1 m , its position is $(-25, 45)$.

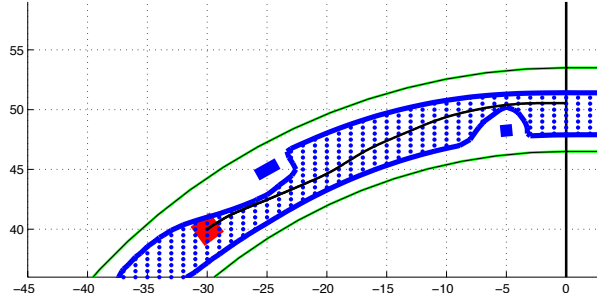


FIGURE 11. (Scenario 3a) Reachable set \mathcal{R}_5 for a curved road with two fixed obstacles.

Scenario 3b: In this scenario depicted in Figure 12, the road parameters are similar, there is now only one obstacle but that is furthermore moving with a circular motion at speed of 5 m s^{-1} .

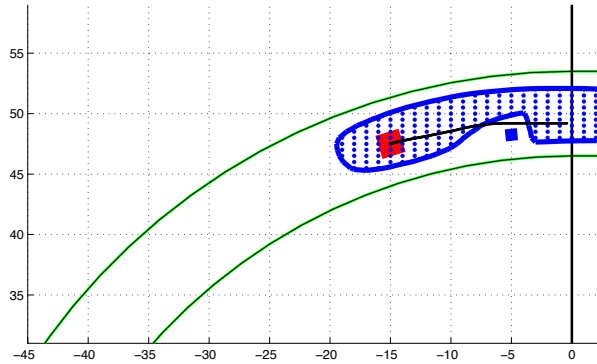


FIGURE 12. (Scenario 3b) Reachable set \mathcal{R}^f for a curved road with one moving obstacle.

5.4. Scenario 4: crossing road and moving obstacles. The following scenario involves a crossing. As in (22) the width of the four streets involving a crossing can be different one from each other.

Here, the horizontal lower and upper road bounds and the vertical limits are different, as illustrated in Fig.13. An object (blue rectangle) of dimensions 1 m is traveling from left to right from position $(-10.0, -2.0)$ meters with speed 5 m s^{-1} and deceleration 5 m s^{-2} . A second obstacle (length 1.0 m and width 2.0 m) starting from position $(-18, 4)$ is traveling from top to bottom with speed 5 m s^{-1} and deceleration 5 m s^{-2} . Within time $t_f = 2.5 \text{ s}$ the red square of dimensions 1.0 m has to reach one of the three targets at the end of each road: top (with steering angle $\frac{\pi}{2} \text{ rad}$), bottom (with steering angle $-\frac{\pi}{2} \text{ rad}$) or right (with steering angle 0 rad). At this speed and for an

initial position close to the center of the crossing, the red vehicle is able to leave the crossing before the second obstacle enters the center of the crossing. In this example the optimal trajectory (black line) will steer to avoid the obstacle in the front and will also decelerate to avoid the second obstacle.

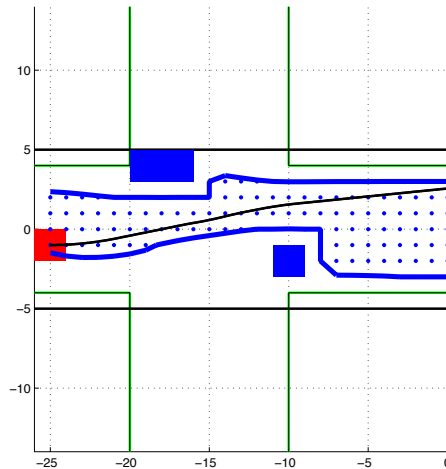


FIGURE 13. (Scenario 4) Reachable set $\mathcal{R}_{2.5}$ for a crossing with one fixed and one moving obstacle.

6. CONCLUSION

We have shown the feasibility of the HJB approach for computing safety regions for some vehicle collision avoidance problems. A 4-dimensional "point mass" model was used to describe the vehicle. The HJB approach turns out to be very powerful especially for complicated road geometries and multiple obstacles. A next and challenging step would be to analyze the present approach using more precise models, such as the so-called 7-dimensional "single track" model. Ongoing works also concern the sensitivity of the secure region with respect to small disturbances of the data.

REFERENCES

- [1] J.-P. AUBIN, A. M. BAYEN, P. SAINT-PIERRE, "Viability theory. New Directions", *Systems & Control: Foundations & Applications*, Springer, Heidelberg, second edition, 2011.
- [2] R. BAIER, M. GERDTS, *A computational method for non-convex reachable sets using optimal control*, Proceedings of the European Control Conference (ECC) 2009 in Budapest (Hungary), August 23–26, 2009, EUCA, Budapest, Hungary, (2009), 97–102.
- [3] R. BAIER, M. GERDTS, I. XAUSA, *Approximation of Reachable Sets using Optimal Control Algorithms*, Numer. Algebra Control Optim., 3(3) (2013), 519–548.
- [4] M. BARDI, I. CAPPUZZO-DOLCETTA, "Optimal control and viscosity solutions of Hamilton-Jacobi-Bellman equations, with appendices by M. Falcone and P. Soravia", *Systems and Control: Foundations and Applications*. Birkhäuser Boston, Inc., Boston, MA, 1997.

- [5] BARRON, E. N. AND ISHII, H., “The Bellman equation for minimizing the maximum cost,” *Nonlinear Nanalysis T.M.A.*, Vol 13, 1989, pp. 1067–1090.
- [6] O. BOKANOWSKI, N. FORCADEL, AND H. ZIDANI, *Reachability and minimal times for state constrained nonlinear problems without any controllability assumption*, SIAM J. Control Optim., 48(7) (2010), pp. 4292–4316.
- [7] O. BOKANOWSKI, H. ZIDANI, *Minimal time problems with moving targets and obstacles*, In 18th IFAC World Congress August 28–September 02, 2011 in Milano, Italy, Vol. 18, Part 1, International Federation of Automatic Control, Milano, Italy, (2011), pp. 2589–2593.
- [8] A. DÉSILLES, H. ZIDANI, AND E. CRÜCK, *Collision analysis for an UAV*, In Proceedings of AIAA Guidance, Navigation, and Control Conference 2012 (GNC-12) 13–16 August 2012 in Minneapolis, Minnesota, American Institute of Aeronautics and Astronautics, AIAA 2012-4526, 2012, 23 pages.
- [9] M. FALCONE, AND P. SORAVIA, *Appendix A. Numerical Solution of Dynamic Programming Equations by M. Falcone. Appendix B. Nonlinear \mathcal{H}_∞ Control by P. Soravia*, In M. Bardi, I. Cappuzzo-Dolcetta, Optimal control and viscosity solutions of Hamilton-Jacobi-Bellman equations, Birkhäuser Boston, Inc., Boston, MA, 1997, pp. 471–574.
- [10] P.-A. FAYOLLE, A. PASKO, AND B. SCHMITT, *SARDF: Signed approximate real distance functions in heterogeneous objects modeling*, in Lecture Notes in Comput. Sci., vol. 4889, Springer-Verlag, Berlin, Heidelberg, 2008, pp. 118–141.
- [11] M. GERDTS, *Solving mixed-integer optimal control problems by branch&bound: a case study from automobile test-driving with gear shift control problems*, Optimal Control Appl. Methods, 26(1) (2005), pp. 1–18.
- [12] M. GERDTS, *A variable time transformation method for mixed-integer optimal control problems*, Optimal Control Appl. Methods, 27(3) (2006), pp. 169–182.
- [13] M. GERDTS, *OCPID-DAE1 Optimal Control and Parameter Identification with Differential-Algebraic Equations of Index 1*, User’s Guide, Version 1.3, March 20, 2013, <http://www.optimal-control.de/>.
- [14] M. GERDTS, AND I. XAUSA, *Avoidance Trajectories Using Reachable Sets and Parametric Sensitivity Analysis*, System Modeling and Optimization, 25th IFIP TC 7 Conference, CSMO 2011 in Berlin, Germany, September 12–16, 2011. Revised Selected Papers, Springer, Berlin–Heidelberg, (2013), pp. 491–500.
- [15] J. C. HART, *Sphere tracing: a geometric method for the antialiased ray tracing of implicit surfaces*, The Visual Computer, 12(10) (1996), pp. 527–545.
- [16] I. M. MITCHELL, A. M. BAYEN, AND C. J. TOMLIN. *A time-dependent Hamilton-Jacobi formulation of reachable sets for continuous dynamic games*, IEEE Trans. Automat. Control, 50(7) (2005), pp. 947–957.
- [17] S. OSHER AND C-W. SHU. *High essentially nonoscillatory schemes for Hamilton-Jacobi equations*, SIAM J. Numer. Anal. (1991), 28(4), pp. 907–922.
- [18] O. BOKANOWSKI, A. DESILLES, AND H. ZIDANI. *User’s Guide for the ROC-HJ Solver. Finite Differences and Semi-Lagrangian methods*, Version 1.0, February 2013, <http://uma.ensta-paristech.fr/files/ROC-HJ/>
- [19] I. XAUSA, R. BAIER, M. GERDTS, M. GONTER, AND C. WEGWERTH, *Avoidance trajectories for driver assistance systems via solvers for optimal control problems*, In Proceedings of the 20th International Symposium on Mathematical Theory of Networks and Systems (MTNS), July 9–13, 2012 in Melbourne, Australia, Think Business Events, Melbourne, Australia, (2012), Paper No. 294, 8 pages.

CHAIR OF APPLIED MATHEMATICS, UNIVERSITY OF BAYREUTH,
95440 BAYREUTH, GERMANY. EMAIL: ROBERT.BAIER@UNI-BAYREUTH.DE

LABORATOIRE JACQUES-LOUIS LIONS, UNIVERSITÉ PARIS-DIDEROT
(PARIS 7) UFR DE MATHÉMATIQUES - BÂT. SOPHIE GERMAIN, 5 RUE
THOMAS MANN, 75205 PARIS CEDEX 13. EMAIL: BOKA@MATH.JUSSIEU.FR

INSTITUT FUER MATHEMATIK UND RECHNERANWENDUNG, FAKUL-
TAET FUER LUFT- UND RAUMFAHRTTECHNIK, UNIVERSITAET DER
BUNDESWEHR MUENCHEN, D-85577 NEUBIBERG/MUENCHEN, GERMANY.
EMAIL: MATTHIAS.GERDTS@UNIBW.DE